Journal of Applied Physics

High-performance multiple-doped In_2O_3 transparent conductive oxide films in near-infrared light region

Cite as: J. Appl. Phys. **132**, 135301 (2022); https://doi.org/10.1063/5.0103270
Submitted: 15 June 2022 • Accepted: 06 September 2022 • Published Online: 03 October 2022

Shuyi Chen, Fanying Meng, Jianhua Shi, et al.

Journal of Applied Physics ARTICLE scitation.org/journal/jap

High-performance multiple-doped In_2O_3 transparent conductive oxide films in near-infrared light region

Cite as: J. Appl. Phys. **132**, 135301 (2022); doi: 10.1063/5.0103270
Submitted: 15 June 2022 · Accepted: 6 September 2022 ·
Published Online: 3 October 2022

Shuyi Chen,[1,2] Fanying Meng,[1,2,a)] Jianhua Shi,[1] Zhu Yan,[1,2] Yiyang Liu,[1,2] and Zhengxin Liu[1,2]

AFFILIATIONS

[1]Research Center for New Energy Technology (RCNET), Shanghai Institute of Microsystem and Information Technology (SIMIT), Chinese Academy of Sciences (CAS), Jiading, Shanghai 201800, People's Republic of China
[2]College of Materials Science and Opto-Electronic Technology, University of Chinese Academy of Sciences (UCAS), Shijingshan, Beijing 100049, People's Republic of China

[a)]**Author to whom correspondence should be addressed:** fymeng@mail.sim.ac.cn

ABSTRACT

High-quality W, Mo, Ti, Zr, and Ga-doped indium oxide (multiple-doped In_2O_3) films are deposited at room temperature by direct current magnetron sputtering process under different oxygen proportion, with 200 °C annealing. A maximum Hall mobility of 71.6 $cm^2\ V^{-1}\ s^{-1}$ is obtained at a middle oxygen proportion of 2%, thanks to the reduction of impurity scattering center, which is nearly three times higher than an ITO film of 23.6 $cm^2\ V^{-1}\ s^{-1}$. The multiple-doped In_2O_3 films showed a remarkable 30% improvement of the optical transmittance (>80%) in the near-infrared (NIR) region compared to the ITO film (about 60%), which is mainly attributed to the decrement of free carrier absorption due to low carrier concentration ($<2\times10^{20}\ cm^{-3}$), an order magnitude lower than the ITO film ($1.56\times10^{21}\ cm^{-3}$). Additionally, x-ray diffraction results confirm that the films have a polycrystalline structure with preferential orientation growth in the <100> direction. In the NIR region, the multiple-doped In_2O_3 films have a superior figure of merit of $5.02\times10^{-3}\ \Omega^{-1}$, which is an order magnitude higher than the ITO film ($5.31\times10^{-4}\ \Omega^{-1}$). This work reports a new In_2O_3-based material with both high electrical and optical performance, which is suitable for the application of advanced optoelectronic devices.

I. INTRODUCTION

In recent years, transparent conducting oxide (TCO) films with unique properties of low electrical resistivity and high optical transmittance have attracted considerable interest due to their various applications in optoelectronic devices including light-emitting diodes, solar cells, and liquid crystal displays.[1,2] In_2O_3-based thin films have been widely studied and Sn-doped In_2O_3 (ITO) has become a dominant transparent electrode in the market owing to its low resistivity of $\sim10^{-4}\ \Omega$ cm and high visible light transmittance greater than 80%.[3–5] However, the high carrier concentration of ITO films restricts the transmittance in the near-infrared (NIR) region caused by free carrier absorption (FCA), which limits their applications.[6] Since resistivity depends on the reciprocal of the product of mobility and carrier concentration, low resistivity for transparent conductive films could be guaranteed by high mobility under relatively low carrier concentration conditions, without sacrificing transparency. Hence, to optimize optical transparency, high mobility of TCO films is required to achieve low resistivity with low carrier concentration.

Numerous efforts have been dedicated to obtain high mobility TCO films and metal doping has been demonstrated to be an effective way.[7–9] Compared with ITO films, In_2O_3 films doped with transition metal (W, Mo, Zr, Ti) impurities exhibit greater carrier mobility and better optical properties in the near-infrared region.[10–13] The addition of Zr and W is expected to increase the formation energy of oxygen vacancy and reduce their concentration compared to ITO, for the reason that the standard formation enthalpies per mole of metal of WO_3 and ZrO_2 are lower than those of SnO_2 and In_2O_3.[14] In addition, the substituted Ga^{3+} ions on In^{3+} sites in In_2O_3 lattice cannot be ionized impurity scattering

centers and the carrier concentration is suppressed by the Ga doping which is strongly bonded to oxygen atoms.[15] However, most of these high-performance TCO films were fabricated at high temperature, which imposes restrictions on their applications.[4] Meanwhile, more and more attention has been paid to co-doping and multiple-doping processes in which two or more elements are doped into In_2O_3 simultaneously, such as In_2O_3:Zr,Ti,Ga and In_2O_3:W,Ti,[14,16] and multiple-doping has the potential to enhance the electrical properties and transparency of indium based oxide films.[17] Among various deposition techniques, the direct current (DC) magnetron sputtering[18] method is widely available for the growth of high-quality transparent conductive films.

In this work, W, Mo, Ti, Zr, and Ga elements were served as dopants in In_2O_3-based materials in order to develop high-performance TCO films with high optical transmittance and low resistivity. The multiple-doped In_2O_3 films were fabricated via the DC magnetron sputtering method at room temperature followed by 200 °C air annealing. The functions of oxygen proportion in adjusting the microstructural, electrical, and optical properties of multiple-doped In_2O_3 films were systematically investigated. Compared with conventional ITO films, it was found that our multiple-doped In_2O_3 films exhibit more excellent mobility and higher transmittance in the NIR region. Furthermore, it was discovered that ionized and neutral impurity scattering is the predominant mechanism to confine the mobility of our films. By moderating appropriate oxygen proportion, an excellent transparent conductive film can be acquired.

II. EXPERIMENTAL SECTION

In the experiment, the multiple-doped In_2O_3 films were prepared onto glass substrates (Corning 7059) by DC magnetron sputtering at room temperature. The substrates were immersed in acetone, ethyl alcohol, and de-ionized water of an ultrasonic bath for 15 min, and then dried with nitrogen. Before various gases entered the chamber, the background pressure was kept constant at around 9×10^{-4} Pa. High-purity Ar and O_2 gases were introduced into the chamber and the pressure was maintained at 0.45 Pa. The oxygen proportion of $O_2/(Ar + O_2)$ was varied from 0.5% to 4% to optimize the performance of multiple-doped In_2O_3 films. The 6-in. ceramic target (made by Luoyang Jinglian Photoelectric Materials Co., Ltd) was made of indium oxide doped by 0.3 wt. % WO_3, 0.5 wt. % MoO_3, 0.6 wt. % TiO_2, 1.0 wt. % ZrO_2, and 0.6 wt. % Ga_2O_3 with a purity of 99.99%. For comparison, the same size ITO target with a doping ratio of In_2O_3:SnO_2 equal to 97:3 was fabricated at an oxygen proportion of 2%. The angle between the tray plane and the target plane was 30°, and the distance between the center of the tray and the target was 110 mm. The sputtering power was set at 120 W with a power density of 0.66 W/cm^2, and the tray rotation speed was kept at 2000 r/h. The thickness of the multiple-doped In_2O_3 films was controlled at approximately 110 nm and all the samples were annealed at 200 °C in an air atmosphere for 30 min.

The microstructural properties of these films were characterized via x-ray diffraction (XRD, Rigaku D/max 2200/PC) with Cu-Kα radiation source ($\lambda = 0.154\,05$ nm) and θ–2θ scan mode under an applied voltage of 40 kV with diffraction angle ranging from 10° to 70°. The electrical properties were monitored by Hall-effect measurement (Ecopia HMS-5300 system) with van der Pauw configuration from 80 K to room temperature using a closed liquid nitrogen cryostat. A Uv-Vis-NIR spectrophotometer (Perkin-Elmer Lambda 950) was utilized to acquire optical transmission and reflection spectra at a wavelength range from 300 to 2500 nm. The thickness and optical constant were evaluated by a spectroscopic ellipsometer (SE, J.A. Woollam Co., Inc. M-2000) with Drude, Gaussian, and Tauc–Lorentz models. All the samples were characterized by glass substrates.

III. RESULTS AND DISCUSSION

A. Crystallite structure of multiple-doped In_2O_3 films

The XRD patterns of multiple-doped In_2O_3 films with various oxygen proportion after 200 °C annealing is shown in Fig. 1(a). It can be seen that the annealed multiple-doped In_2O_3 thin films exhibit six peaks of indices (211), (222), (400), (431), (440), and (622), which are well matched with In_2O_3 powder data (JCPDS No. 06-0416). There is no evidence of additional phase related to dopants in the films due to the low doping content, confirming that dopants have been successfully doped into the In_2O_3 crystal lattice without distracting from the cubic structure of In_2O_3. With the increase in oxygen proportion, a decrease in the peak intensity of (222) is observed, while the intensity of (400) is enhanced. The intensity ratio of $I_{(400)}/I_{(222)}$ increases with oxygen proportion as shown in Fig. 1(b), which is larger than the standard values in JCPDS No. 06-0416 (0.3), indicating a preferential orientation growth in the <100> direction. The ITO film also has a preferential orientation to <100> and a lower peak intensity than the multiple-doped In_2O_3 films that manifest a lower degree of crystallinity.

B. Electrical properties of multiple-doped In_2O_3 films

The electrical properties of the multiple-doped In_2O_3 films are analyzed by Hall-effect measurements. Figure 2 illustrates the carrier concentration, mobility, and resistivity of the 200 °C post-annealed multiple-doped In_2O_3 films as a function of the oxygen proportion measured at room temperature. It is clear that the values of the Hall parameters of multiple-doped In_2O_3 films are very sensitive to oxygen proportion. The carrier concentration of post-annealed films initially decreases a little from 3.59×10^{20} to 3.18×10^{20} cm^{-3} as oxygen proportion continuously enhances from 0.5% to 2% and then decreases abruptly to 7.93×10^{19} cm^{-3} at an oxygen proportion of 4%, which is an order of magnitude lower than ITO. The free carriers of the multiple-doped In_2O_3 films are generated by oxygen vacancies (V_O) and metal substitution of In^{3+} by W^{6+}, Mo^{6+}, Ti^{4+}, and Zr^{4+}. Each V_O donates two electrons, W^{6+} and Mo^{6+}, that can, respectively, supply three extra electrons, and Zr^{4+} and Ti^{4+} will each release an electron when replacing In^{3+}. Even at a high oxygen proportion, W^{6+} or Mo^{6+} substituting for In^{3+} will contribute one electron after it associates with one interstitial O^{2-}.[10,19] According to the downward trend in carrier concentration with increasing oxygen proportion, it could be inferred that the change of carrier concentration is strongly correlated with V_O and much more V_O generates higher carrier concentration at low oxygen proportion due to oxygen deficiencies. However, the

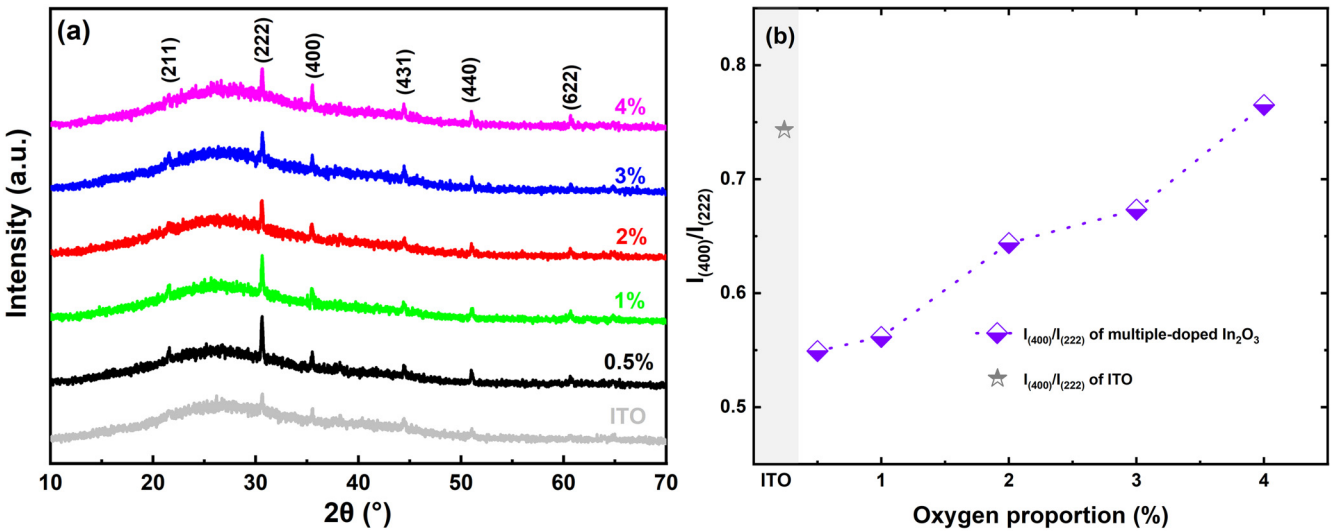

FIG. 1. (a) XRD pattern of the ITO film and the multiple-doped In_2O_3 films with various oxygen proportion. (b) Intensity ratio of $I_{(400)}/I_{(222)}$ of ITO films and multiple-doped In_2O_3 films as a function of oxygen proportion.

incorporation of excess oxygen will recover the oxygen vacancies and deactivate the substituted ions by forming interstitial O^{2-} and associating with doping cation to form electrically neutral complexes, such as $(2W_{In}^{3+}–3O_i^{2-})$,[10] $(2Mo_{In}^{3+}–3O_i^{2-})$,[19] and $(2Ti_{In}^{+}–O_i^{2-})$,[20] leading to the sustained reduction of carrier concentration. The neutral complexes are also detrimental to mobility, as discussed later.

The maximum mobility of multiple-doped In_2O_3 films deposited at a 2% oxygen proportion is 71.6 $cm^2\,V^{-1}\,s^{-1}$, nearly three times higher than the ITO film of 23.6 $cm^2\,V^{-1}\,s^{-1}$. A general trend of decreasing mobility with increasing electron concentration is observed between our multiple-doped In_2O_3 films and ITO films, and this is likely due to the increased ionized impurities scattering, which could be explained by Lewis acid strength. The Lewis acid strength L is defined by Zhang[21] as follows:

$$L = \frac{Z}{r^2} - 7.7\chi_z + 0.8, \tag{1}$$

where r is the ionic radius and χ_z is the electronegativity of the element in the respective oxidation state Z. According to the study of Wen *et al.*,[22] the high Lewis acid dopants polarize the electronic charge away from the O^{2-} 2p valence band more strongly than weaker Lewis acids. This results in screening of the charge and weakens its activity as a scattering center, hence increasing the mobility. Compared to the Lewis acid strength of In^{3+} (1.026) and Sn^{4+} (0.228), the dopants in our multiple-doped In_2O_3 films possess higher Lewis acid strengths such as W^{6+} (3.158), Mo^{6+} (3.667), Ti^{4+} (3.064), and Zr^{4+} (2.043),[23] meaning less impurities scattering and higher mobility.

The oxygen proportion obviously has an effect on the mobility of multiple-doped In_2O_3 films. The carrier mobility of the multiple-doped In_2O_3 films first increases with increasing oxygen proportion and reaches the maximum Hall mobility of 71.6 $cm^2\,V^{-1}\,s^{-1}$ at an oxygen proportion of 2%, then reduces to 1.62 $cm^2\,V^{-1}\,s^{-1}$ with further increasing the oxygen proportion to 4%. The change of carrier mobility in multiple-doped In_2O_3 films with oxygen proportion is related to scattering mechanisms, such as ionized and neutral impurity scattering, thermal lattice vibration scattering, and grain boundary scattering.[24] In order to verify the effect of oxygen proportion on the electron transport property of multiple-doped In_2O_3 films, the temperature dependence of carrier mobility is measured in a range from 80 to 300 K, as illustrated in Fig. 3. For films deposited at low oxygen proportion from 0.5% to 2%, the decrement in carrier mobility with heating up from 150 to 300 K is indicative of the existence of lattice (phonon) scattering. Ionized and neutral impurity scattering is independent of temperature in degenerate semiconductors, whereas phonon scattering approximatively follows a power law: $\mu \propto T^{-p}$.[25] We determine $0.24 \le p \le 0.47$ for multiple-doped In_2O_3 films, which is consistent with previous experiments in doped In_2O_3 films.[26,27] Although the phonon scattering can be neglected, the mobility of films deposited at high oxygen proportion is not satisfactory due to heavy ionized/neutral impurity scattering. We could deduce that oxygen vacancies are gradually occupied with increasing oxygen content at low oxygen proportion and the decrease of scattering centers V_O gives rise to the boost of mobility, while excess oxygen will associate with substitutional metal dopants to form neutral complexes and contributes to the reduction of mobility. Besides, grain boundary barrier heights depend sensitively on carrier concentration and increase with decreasing carrier concentration, which is a factor that limits the mobility in films with lower carrier concentration at high oxygen proportion ($<10^{20}$ cm^{-3}).[28,29]

We would like to point out that the resistivity of multiple-doped In_2O_3 films is sensitive to the oxygen content during

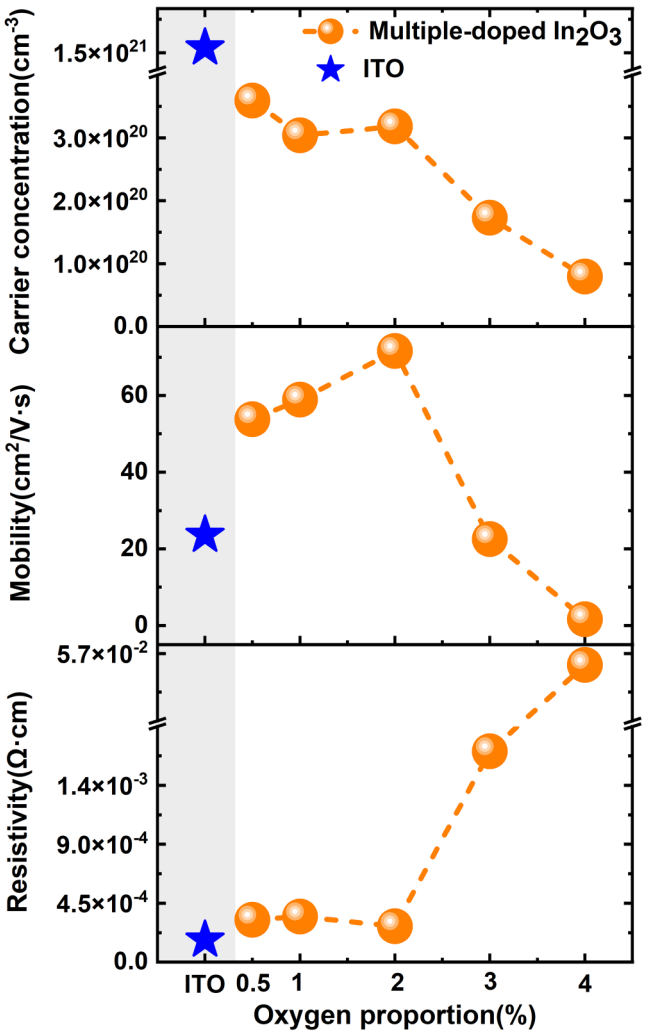

FIG. 2. Room-temperature Hall-effect measurements for the multiple-doped In_2O_3 films as a function of oxygen proportion.

deposition and the films with low resistivity are only achieved in a short range of oxygen proportion (0.5%–2%). The minimum resistivity of multiple-doped In_2O_3 films reaches $2.74 \times 10^{-4}\,\Omega\,\mathrm{cm}$, which is comparable to ITO. Based on the above analysis, we demonstrate that the electrical properties of multiple-doped In_2O_3 films are not inferior to ITO films.

C. Optical properties of multiple-doped In_2O_3 films

Figure 4 displays the optical transmittance and reflectance spectra of the 200 °C post-annealed multiple-doped In_2O_3 films and the contrast ITO spectrum is also shown in a gray dash line. It is obvious that oxygen proportion plays an important role in the optical property of multiple-doped In_2O_3 films. Low average transmittance of 70.3% is obtained when oxygen is insufficient, and the

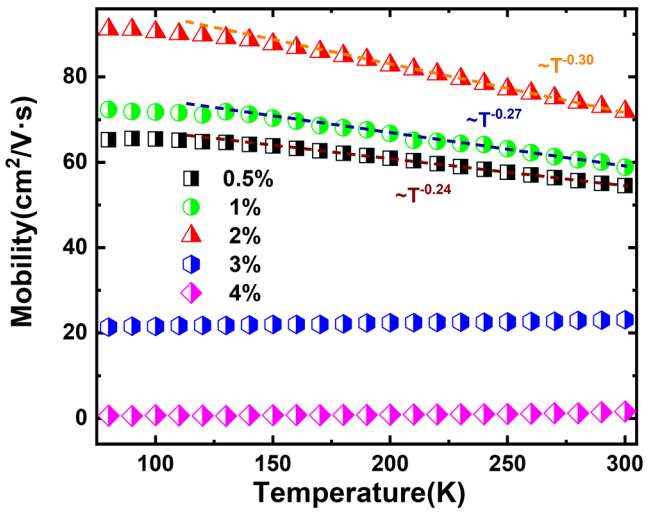

FIG. 3. Variation of Hall mobility as a function of temperature for the multiple-doped In_2O_3 films fabricated with different oxygen proportion between 80 and 300 K. The dashed line qualitatively represents asymptotic mobility due to optical phonon scattering only.

average transmittance increases rapidly over 80% when increasing oxygen proportion to 2% and more. It clearly shows that increasing oxygen proportion enhances the transmittance of multiple-doped In_2O_3 films within the visible region from 400 to 700 nm and the NIR region from 1600 to 2500 nm. The average transmittance increases from 69.8% to 84.5% in the visible region and from 71.1% to 85.5% in the NIR region with an increasing oxygen proportion from 0.5% to 4%. The optical transmittance of ITO films is

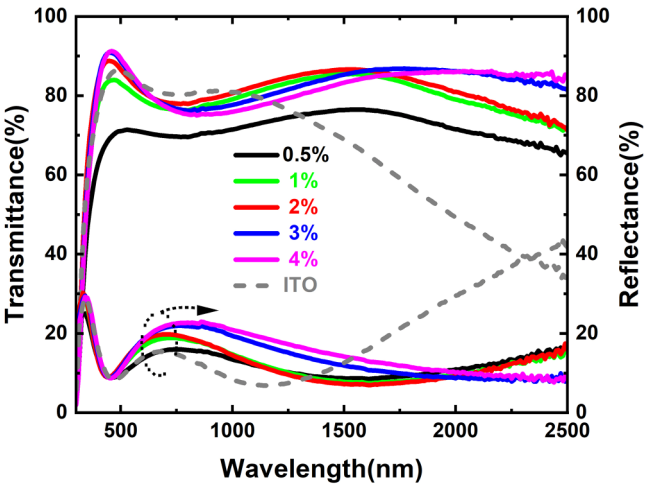

FIG. 4. Optical transmittance and reflectance spectra of multiple-doped In_2O_3 films with various oxygen proportion and ITO films.

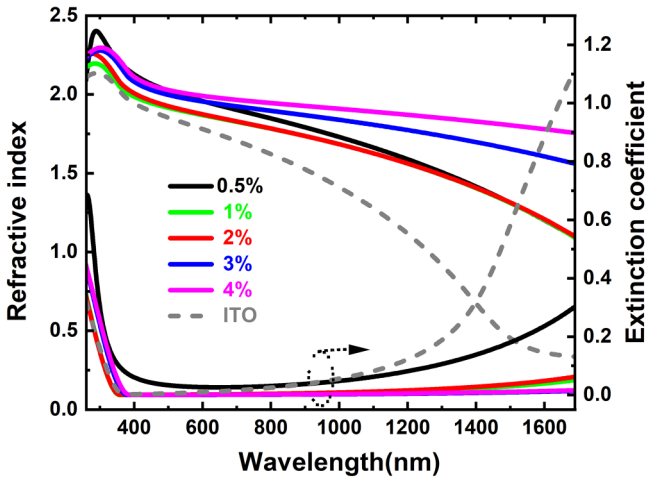

FIG. 5. Refractive index and extinction coefficient curves of multiple-doped In_2O_3 films with various oxygen proportion and ITO films.

only 48.2% from 1600 to 2500 nm. Obviously, the transmittance of multiple-doped In_2O_3 films is absolutely superior to conventional ITO films in the infrared wavelength region, which is ascribed to the reduction in free carrier absorption (FCA).[6] As shown in Fig. 2, the carrier concentration of multiple-doped In_2O_3 films is lower than ITO films and falls down with the increase in oxygen proportion, leading to the weakening of FCA effect, which is favorable to the transmittance of multiple-doped In_2O_3 films in the NIR region.

Figure 5 presents the optical constants (refractive index n and extinction coefficient k) of multiple-doped In_2O_3 films and the ITO film after 200 °C annealing. Obviously, the film deposited at 0.5% has a large absorption in the visible and NIR regions, while the films deposited at higher oxygen proportion are almost transparent. The multiple-doped In_2O_3 films deposited at higher oxygen proportion feature higher n and lower k in the NIR region. Extinction coefficient increases with the decrease in refractive index due to the high carrier concentration in the long wavelength region, which leads to the FCA effect as discussed before. It is found that the multiple-doped In_2O_3 films with high oxygen proportion have

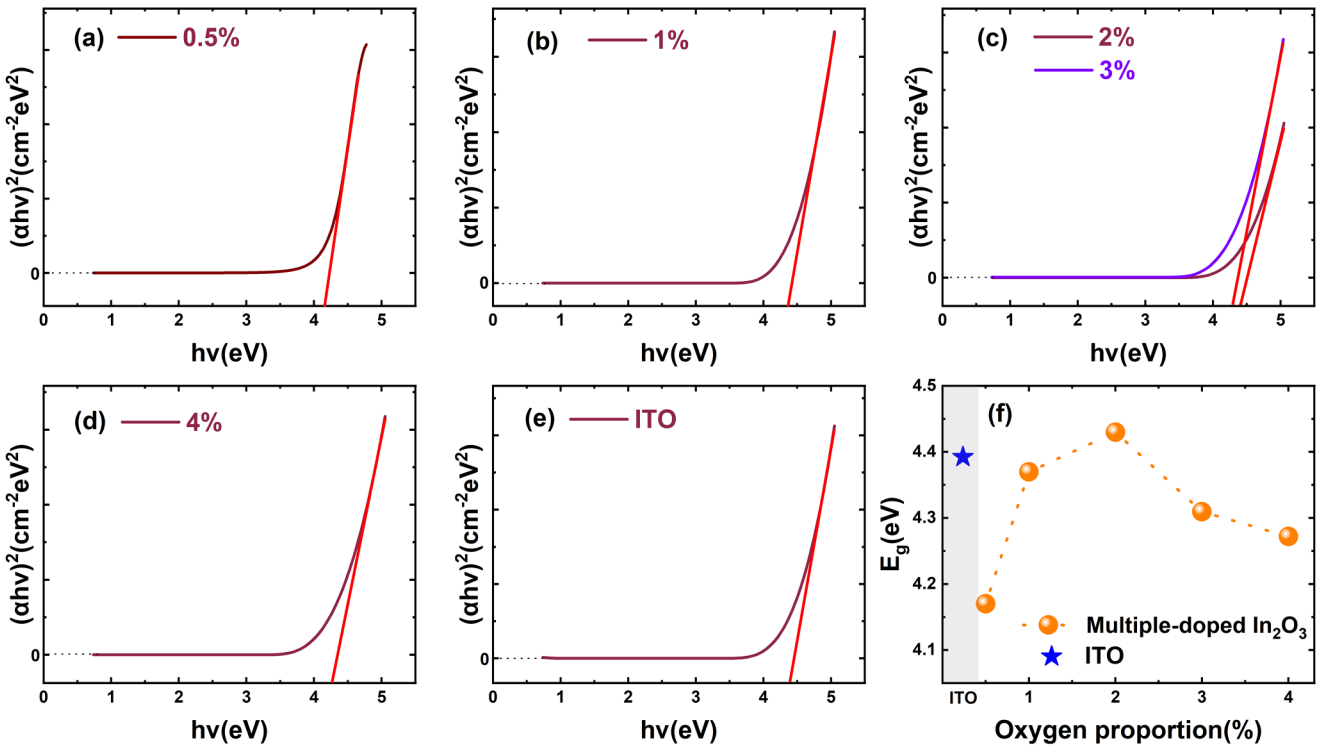

FIG. 6. The $(\alpha h\nu)^2$ spectra and their linear extrapolation for multiple-doped In_2O_3 films at an oxygen proportion of (a) 0.5%, (b) 1%, (c) 2% and 3%, and (d) 4%; (e) ITO for comparison; (f) the plot of optical bandgap (E_g) of multiple-doped In_2O_3 films as a function of the oxygen proportion.

higher n and lower k compared to the ITO film, especially in the NIR region. It is worth noting that although k of the multiple-doped In_2O_3 films at high oxygen proportion increases with wavelength, it is still at a relatively low level.

The optical bandgap (E_g) of multiple-doped In_2O_3 films is determined from extinction coefficient data. The absorption coefficient (α) is calculated using the relation $\alpha = 4\pi k/\lambda$, where k is the extinction coefficient and λ is the wavelength of the incident light. The relation between incident photon energy ($h\upsilon$) and the absorption coefficient is given by Tauc's law,[4]

$$(\alpha h\upsilon)^2 = A(h\upsilon - E_g), \tag{2}$$

where A is a constant. Figure 6 exhibits the $(\alpha h\upsilon)^2$ spectra and their linear extrapolation for multiple-doped In_2O_3 films at different oxygen proportion and the ITO film for comparison, whereas (f) is the plot of the optical bandgap as a function of the oxygen proportion. It is observed that the E_g values increase with the increase in oxygen proportion and reach a higher value of 4.43 eV for films deposited at 2% oxygen proportion. As oxygen proportion further increases, the E_g values slightly decrease and reach 4.27 eV at an oxygen proportion of 4%. The variation trend for the bandgap of multiple-doped In_2O_3 films should consider both bandgap narrowing and the Burstein–Moss effect. When excess oxygen vacancies exist at low oxygen proportion, the oxygen vacancy states become nonlocalized and overlap with the valence band edge, raising the position of the valence band, and leading to the narrowing of the bandgap.[30,31] Nevertheless, the reduction of the bandgap at high oxygen proportion with lower carrier concentration can be explained by the Burstein–Moss effect, the band filling effect is weakened with the decrease in carrier concentration.[32] The deeper mechanism in multiple-doped In_2O_3 films should be further investigated.

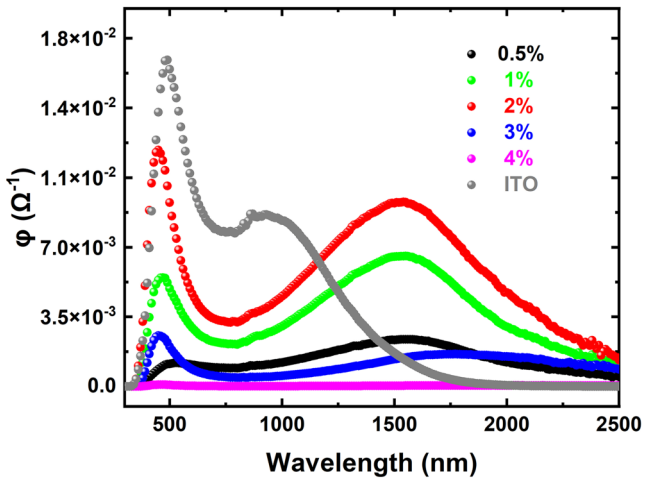

FIG. 7. Plot of the figure of merit (φ) vs wavelength for the multiple-doped In_2O_3 films and ITO films.

TABLE I. Average figure of merit of the multiple-doped In_2O_3 films and ITO film deposited at various oxygen proportion in the visible and the NIR regions.

	Figure of merit, φ (Ω^{-1})	
Oxygen proportion (%)	Visible region (400–780 nm)	NIR region (800–2500 nm)
0.5	9.49×10^{-4}	1.35×10^{-3}
1	3.20×10^{-3}	3.43×10^{-3}
2	5.60×10^{-3}	5.02×10^{-3}
3	1.02×10^{-3}	1.06×10^{-3}
4	3.40×10^{-5}	3.24×10^{-5}
ITO	1.02×10^{-2}	5.31×10^{-4}

D. Figure of merit

It is a great challenge to achieve high conductivity and maximum transparency in the same material, so in order to evaluate the performance of multiple-doped In_2O_3 films as transparent conductive electrodes, a figure of merit (φ) is generally used according to Haacke's definition,[33]

$$\varphi = \frac{T^{10}}{R_S}, \tag{3}$$

where R_S is the sheet resistance and T is the optical transmittance. The trend of φ with wavelength is directly visualized in Fig. 7, ITO has higher φ in the visible region due to the lower resistivity of ITO material, and little difference in transmittance between ITO and the multiple-doped In_2O_3 films in the visible region. While the φ of ITO descends rapidly in the NIR region, the multiple-doped In_2O_3 films have superior φ values, especially from 1200 to 2500 nm. It is evident that φ of the multiple-doped In_2O_3 films first increases with the increase in oxygen content and reaches the maximum at an oxygen proportion of 2%, then falls down with further increasing oxygen proportion, no matter in the visible or the NIR region. Table I lists the average φ in the visible and the NIR region, the average maximum φ of the multiple-doped In_2O_3 films in the NIR region from 800 to 2500 nm is $5.02 \times 10^{-3}\ \Omega^{-1}$, which is at least an order of magnitude better than the ITO film of $5.31 \times 10^{-4}\ \Omega^{-1}$. Meanwhile, the transverse difference between the visible and NIR regions of the multiple-doped In_2O_3 films is not remarkable. Therefore, the prepared multiple-doped In_2O_3 thin films in this study demonstrate high figures of merit in a broadband region, which can provide applications for TCO materials that require excellent performance in the infrared wavelength region.

IV. CONCLUSION

In this study, we investigated the influence of oxygen proportion on the structural, electrical, and optical properties of multiple-doped In_2O_3 thin films prepared at room temperature, employing a DC sputtering technique followed by 200 °C post-annealing. The experimental results indicate that the multiple-doped In_2O_3 films possess predominately <100>-oriented crystalline structure. The maximum mobility of 71.6 $cm^2\ V^{-1}\ s^{-1}$ with a carrier concentration

of $3.18 \times 10^{20}\,cm^{-3}$ is acquired at an oxygen proportion of 2%. Compared to high oxygen proportion, besides ionized impurity scattering and/or neutral impurity scattering, the mobility of the multiple-doped In_2O_3 films with insufficient oxygen content is more likely to be impacted by lattice vibration scattering. The films with adequate oxygen feature higher transmittance, higher refractive index, and lower extinction coefficient. The multiple-doped In_2O_3 films have excellent figure of merit values in the NIR region and the average figure of merit from 800 to 2500 nm is up to $5.02 \times 10^{-3}\,\Omega^{-1}$ at an oxygen proportion of 2%. This work reports a high-performance In_2O_3-based TCO material, which is promising for the application of various optoelectronic devices demanding both excellent optical transparency and electrical conductivity in the NIR region.

ACKNOWLEDGMENTS

This work was supported by the Key-Area Research and Development Program of Guangdong Province (No. 2021B0101260001), the Strategic Priority Research Program of Chinese Academy of Sciences (No. XDA17020403), and the Projects of Science and Technology Commission of Shanghai (Nos. 17DZ1201100 and 19DZ1207602).

AUTHOR DECLARATIONS

Conflict of Interest

The authors have no conflicts to disclose.

Author Contributions

Shuyi Chen: Conceptualization (equal); Investigation (equal); Methodology (equal); Writing – original draft (equal). **Fanying Meng:** Conceptualization (equal); Project administration (equal); Supervision (equal); Validation (equal); Writing – review & editing (equal). **Jianhua Shi:** Validation (equal); Writing – review & editing (equal). **Zhu Yan:** Validation (equal); Writing – review & editing (equal). **Yiyang Liu:** Validation (equal); Writing – review & editing (equal). **Zhengxin Liu:** Funding acquisition (lead); Validation (equal); Writing – review & editing (equal).

DATA AVAILABILITY

The data that support the findings of this study are available from the corresponding author upon reasonable request.

REFERENCES

[1]D. P. Joseph, R. Radha, J. M. Fernandes, R. Muniramaiah, N. Purushothamreddy, M. Kovendhan, and C. Venkateswaran, J. Mater. Sci. Mater. Electron. **33**, 8435–8445 (2022).
[2]T. Jaeger, Y. E. Romanyuk, S. Nishiwaki, B. Bissig, F. Pianezzi, P. Fuchs, C. Gretener, M. Doebeli, and A. N. Tiwari, J. Appl. Phys. **117**, 205301 (2015).
[3]O. Bierwagen, Semicond. Sci. Technol. **30**, 024001 (2015).
[4]M. Ahmed, A. Bakry, A. Qasem, and H. Dalir, Opt. Mater. **113**, 110866 (2021).
[5]D. Wan, P. Chen, J. Liang, S. Li, and F. Huang, ACS Appl. Mater. Interfaces **3**, 4751–4755 (2011).
[6]H. Peelaers, E. Kioupakis, and C. G. Van de Walle, Appl. Phys. Lett. **115**, 082105 (2019).
[7]J. Wang, C. Meng, H. Liu, Y. Hu, L. Zhao, W. Wang, X. Xu, Y. Zhang, and H. Yan, ACS Appl. Energy Mater. **4**, 13586–13592 (2021).
[8]B. A. D. Williamson, T. J. Featherstone, S. S. Sathasivam, J. E. N. Swallow, H. Shiel, L. A. H. Jones, M. J. Smiles, A. Regoutz, T.-L. Lee, X. Xia, C. Blackman, P. K. Thakur, C. J. Carmalt, I. P. Parkin, T. D. Veal, and D. O. Scanlon, Chem. Mater. **32**, 1964–1973 (2020).
[9]R. S. babu, Y. N. murthy, K. Hari Prasad, T. Alshahrani, S. J. McCormack, M. Shkir, and S. AlFaify, Optik **223**, 165408 (2020).
[10]F. Meng, J. Shi, Z. Liu, Y. Cui, Z. Lu, and Z. Feng, Sol. Energy Mater. Sol. Cells **122**, 70–74 (2014).
[11]N. Yamada, M. Yamada, H. Toyama, R. Ino, X. Cao, Y. Yamaguchi, and Y. Ninomiya, Thin Solid Films **626**, 46–54 (2017).
[12]J.-W. Ok, H.-S. Oh, D.-J. Kwak, Y.-M. Sung, and S.-H. Kim, J. Nanosci. Nanotechnol. **15**, 1525–1528 (2015).
[13]T. Koida and M. Kondo, J. Appl. Phys. **101**, 063705 (2007).
[14]T. Koida and J. Nomoto, Phys. Rev. Mater. **6**, 055401 (2022).
[15]K. Ebata, S. Tomai, Y. Tsuruma, T. Iitsuka, S. Matsuzaki, and K. Yano, Appl. Phys. Express **5**, 011102 (2012).
[16]W. Huang, J. Shi, Y. Liu, Z. Wu, F. Meng, and Z. Liu, J. Power Sources **506**, 230101 (2021).
[17]Y. Liu, F. Meng, J. Shi, W. Huang, W. Liu, and Z. Liu, J. Mater. Sci.: Mater. Electron. **32**, 3201–3210 (2021).
[18]Ş. Ţălu , S. Kulesza, M. Bramowicz, K. Stępień, and D. Dastan, Arch. Metall. Mater. **66**, 443 (2021).
[19]C. Warmsingh, Y. Yoshida, D. W. Readey, C. W. Teplin, J. D. Perkins, P. A. Parilla, L. M. Gedvilas, B. M. Keyes, and D. S. Ginley, J. Appl. Phys. **95**, 3831–3833 (2004).
[20]R. Hashimoto, Y. Abe, and T. Nakada, Appl. Phys. Express **1**, 015002 (2008).
[21]Y. Zhang, Inorg. Chem. **21**, 3886–3889 (1982).
[22]S. J. Wen, G. Campet, J. Portier, G. Couturier, and J. B. Goodenough, Mater. Sci. Eng., B **14**, 115–119 (1992).
[23]S. Calnan and A. N. Tiwari, Thin Solid Films **518**, 1839–1849 (2010).
[24]Y.-T. Li, D.-T. Chen, C.-F. Han, and J.-F. Lin, Vacuum **183**, 109844 (2021).
[25]B. Macco, H. C. M. Knoops, and W. M. M. Kessels, ACS Appl. Mater. Interfaces **7**, 16723–16729 (2015).
[26]E. Rucavado, F. Landucci, M. Döbeli, Q. Jeangros, M. Boccard, A. Hessler-Wyser, C. Ballif, and M. Morales-Masis, Phys. Rev. Mater **3**, 084608 (2019).
[27]E. Aydin, M. De Bastiani, X. Yang, M. Sajjad, F. Aljamaan, Y. Smirnov, M. N. Hedhili, W. Liu, T. G. Allen, L. Xu, E. Van Kerschaver, M. Morales-Masis, U. Schwingenschlögl, and S. De Wolf, Adv. Funct. Mater. **29**, 1901741 (2019).
[28]M. V. Frischbier, H. F. Wardenga, M. Weidner, O. Bierwagen, J. Jia, Y. Shigesato, and A. Klein, Thin Solid Films **614**, 62–68 (2016).
[29]Y. Magari, T. Kataoka, W. Yeh, and M. Furuta, Nat. Commun. **13**, 10781078 (2022).
[30]H. Liu, F. Zeng, Y. Lin, G. Wang, and F. Pan, Appl. Phys. Lett. **102**, 181908 (2013).
[31]K. G. Saw, N. M. Aznan, F. K. Yam, S. S. Ng, and S. Y. Pung, PLoS One **10**, e0141180 (2015).
[32]S. Guo, W. Diyatmika, Y. Unutulmazsoy, L. Yang, B. Dai, L. Xu, J. Han, V. Ralchenko, A. Anders, and J. Zhu, Appl. Surf. Sci. **585**, 152604 (2022).
[33]G. Haacke, J. Appl. Phys. **47**, 4086–4089 (1976).